Hydrogenolysis of Carbon and Its Catalysis by Platinum

W. L. HOLSTEIN AND M. BOUDART

Department of Chemical Engineering, Stanford University, Stanford, California 94305

The hydrogenolysis of carbon to methane and its catalysis by platinum were studied above and below 1050 K, respectively. Hydrogen pressure varied between ca. 10 and 100 kPa. At 890 K and atmospheric pressure, platinum accelerated the rate of the uncatalyzed reaction by a factor of 2000. Reaction orders with respect to H_2 and kinetic isotope effects in H_2 and D_2 suggest rapid equilibration of the carbon surface with hydrogen followed by a rate-determining step involving breaking of a carbon–carbon bond. This step appears to be a true hydrogenolysis step with direct participation of hydrogen in the uncatalyzed reaction. But with platinum, the rate-determining step seems to lead to the formation of a carbon–platinum bond with subsequent reaction of the carbidic carbon on platinum.

INTRODUCTION

The reaction between carbon and hydrogen has been studied many times, though not as extensively as other carbon–gas reactions, due to the low reactivity of carbon with hydrogen. Below about 1800 K the predominant product is methane. At higher temperatures, methane becomes unstable relative to carbon and hydrogen and the primary product is acetylene. We will only consider the low-temperature reaction to methane:

$$C + 2H_2 = CH_4.$$
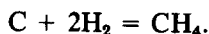
This hydrogenation, or more properly the hydrogenolysis of carbon is limited by equilibrium at low pressures and high temperatures. The equilibrium constant

$$K = P_{CH_4}/(P_{H_2})^2$$

with partial pressures in atmospheres, is 1.41, 0.098, and 0.0162 at 800, 1000, and 1200 K, respectively. The partial pressure of methane in equilibrium with hydrogen decreases rapidly with decreasing hydrogen partial pressure.

The kinetics of the uncatalyzed hydrogenolysis of carbon has been studied be-

tween 1090 and 1525 K at hydrogen pressures from 9,000 to 10,000 kPa (1–6). The reaction orders in hydrogen and activation energies reported in these studies are summarized in Table 1. Reaction orders in hydrogen vary from 0.9 to 2.0, with the exception of one study (6), where reaction orders from 0 to 0.6 were reported. Considering the much lower temperatures at which methane was observed in this latter study, it is likely that the methane is being produced through a different mechanism, perhaps through a catalytic process, as will become apparent below.

Rewick, et al. (7) investigated the kinetics of the platinum-catalyzed hydrogenolysis of Norit A, a vegetable carbon, between 975 and 1175 K at hydrogen pressures from 1 to 101 kPa using a gravimetric balance to record weight changes of carbon. A maximum in the Arrhenius plot was found. At temperatures below the maximum, an activation energy of 230 kJ mol^{-1} and a reaction order of $\frac{1}{2}$ were determined. The authors invoked hydrogen spillover, first proposed by Robell et al. (8) in a study of the platinum-catalyzed adsorption of hydrogen on Spheron, a channel black, at temperatures too low (573–665 K) for methane to be formed. Spillover involves, in succession, dissociative adsorption of

328

TABLE 1

Reaction Orders and Activation Energy, E, for
Uncatalyzed Hydrogenolysis of Carbon

Reference	T (K)	P (kPa)	Reaction Order in H_2	E (kJ mol^{-1})
6	635–790	12–24	0	50
	790–1,065	12–24	0.6	293
5	1,245–1,365	9–64	1.5	90
2	925–1,145	100–4,000	1	125
1	1,090–1,200	1,000–3,000	0.9–1.6	70–210
3	1,275–1,525	1,000–10,000	1	355
4	1,025–1,325	1,000–10,000	1–2	150–330
This study	1,040–1,220	14–101	1.41	215

hydrogen on platinum, migration of hydrogen atoms across the platinum–carbon interface to the carbon surface and diffusion of hydrogen atoms on the carbon surface to reactive sites. Rewick et al. postulated a reaction of hydrogen adsorbed on carbon to form methane at the reactive sites. The rate-determining step was assumed to be the interfacial migration of hydrogen to the carbon. The maximum in rate as a function of temperature was explained as being due to the competition between two surface processes—the formation of a reactive carbon surface for the gasification reaction and thermal annealing of the surface. However, as noted by Marsh and Taylor (9), surface annealing has resulted in maxima in rate for other gas–carbon reactions only at temperatures above 1500 K. It appears unlikely that surface annealing is significant at 1100 K. According to Marsh and Taylor, the maximum in rate resulted from pore diffusion influencing the rate at high temperatures. However, this should only result in a decrease in the measured activation energy—not a negative activation energy.

Following a previous study where no reaction between graphite and hydrogen could be detected (10), Olander and Balooch studied the platinum-catalyzed hydrogenolysis of graphite between 500 and 900 K with a pulsed molecular beam of intensity from 0.6×10^{17} to 6×10^{17} cm^{-2} s^{-1} (11). The production of methane was observed at temperatures as low as 525 K.

A maximum in the reaction rate with temperature was observed at 683 K. The results were fitted by an optimization code to a spillover model with 10 adjustable parameters. Their results cannot be used as evidence that catalyzed carbon hydrogenolysis occurs via reaction of spilled-over hydrogen due to the large number of adjustable parameters and due to the fact that the model employed allows for the direct desorption of hydrogen from graphite but not for the direct adsorption of hydrogen on graphite. This is a violation of the principle of microscopic reversibility, because for the production of methane from hydrogen and carbon to occur, there must be a sequence of elementary steps for which the affinity of each of the elementary steps is greater than zero. If the affinity for each of the steps leading to the adsorption of hydrogen on carbon via hydrogen spillover is greater than zero, then the affinity for the direct adsorption of hydrogen on carbon must also be greater than zero and the direct adsorption of hydrogen on carbon must occur at a faster rate than the direct desorption of hydrogen from carbon.

Tomita et al. studied the hydrogenolysis of active carbon catalyzed by several metals at atmospheric pressure using a gravimetric balance at increasing (12) or constant temperatures (13). Thermogravimetric studies yielded peaks in reaction rate as a function of temperature for platinum-catalyzed hydrogenolysis at 1045 and 1275 K, while studies made at constant temperature yielded a peak at 1055 K. An activation energy of 150 kJ mol^{-1} was calculated for the reaction at low temperatures.

Investigation performed to date yield conflicting activation energies for both the uncatalyzed and platinum-catalyzed hydrogenolysis of carbon. It is generally agreed that the uncatalyzed reaction is 1 to $\frac{3}{2}$ order in hydrogen. A maximum in reactivity with temperature for the platinum-catalyzed hydrogenolysis has been found in several investigations.

Before the mechanism of the uncatalyzed or catalyzed reactions can be understood, discrepancies in the kinetics should be explained. The purpose of the present study was to clarify kinetics prior to a mechanistic study still under way.

EXPERIMENTAL

The carbon selected was Spheron 6, a high-purity (99.95%) channel black made by the Godfrey Cabot Corporation. Spheron 6 was selected because of its purity and high specific surface area. It consists of almost spherical nonporous particles 15 nm in radius. The 1% Pt/Spheron samples, referred to as Pt/C, were prepared by impregnation of the carbon with chloroplatinic acid dissolved in 95% ethanol using incipient wetness. The impregnated carbon was then dried at 343 K for several hours (14).

Hydrogen was purified by diffusion through palladium, although identical rates were observed for purified and unpurified hydrogen. Deuterium (Matheson, 99.5%) and helium (99.995%) were used as received.

In all runs, the same weight (5 g) of carbon or 1% Pt/C was charged into a quartz fixed-bed reactor contained in a high-temperature furnace (15). The sample was pretreated at 1225 K in flowing helium at atmospheric pressure for 2 hr to remove adsorbed surface oxides present on the carbon surface and provide a reproducible state for kinetic measurements.

Hydrogenolysis data were obtained by flowing hydrogen/helium mixtures of known composition at a rate of 5.5 l(STP) h^{-1} through the packed bed of carbon at reaction temperature and measuring the concentration of methane in the gas leaving the reactor with a gas chromatograph equipped with a thermal conductivity detector employing a helium carrier gas. Methane was separated from hydrogen by a $\frac{1}{4}''$ Poropak Q column 6 ft in length maintained at 333 K. The gas chromatograph was calibrated for methane using a 1.08%

methane/helium calibrating gas obtained from Matheson. The gas chromatograph was calibrated for deuterated methane by comparing peak heights produced by injecting samples of 1.37, 3.64, and 9.67% CD_4/helium and CH_4/helium. The peak heights for methane and deuterated methane were identical within an experimental error of 2%.

The reactor was operated differentially, that is, the conversion of hydrogen was kept below 5%. Thus the hydrogen concentration was effectively constant through the carbon bed. Kinetic isotope effect results were obtained by the following procedure. Hydrogen was flowed through the packed bed of carbon and the rate of production of methane was measured. The hydrogen flow was stopped and deuterium was flowed through the bed at the same flow rate. After a period of at least 10 min the production rate of deuterated methane was measured. The procedure was reversed and the production of methane was again measured. The rates of reaction for hydrogen were the same before and after the deuterium was flowed through the bed.

RESULTS

The initial BET surface area was 102 m^2 g^{-1} for the carbon and 91 m^2 g^{-1} for the 1% Pt/C. After pretreatment of the latter, the dispersion of the platinum was 48% by hydrogen titration of preadsorbed oxygen (16). No attempt was made to follow the changing surface area of the carbon or the changing dispersion of platinum during the course of the reaction. All rates are re-

TABLE 2

Rates r and r' of the Uncatalyzed Reaction of Carbon in H_2 and D_2, Respectively

T (K)	r (ng m^{-2} s^{-1})	r' (ng m^{-2} s^{-1})	r/r'
1134	1.80	1.61	1.12
1191	4.91	4.40	1.11
			1.12 ± 0.05

TABLE 3

Rates r and r' of the Pt-Catalyzed Reaction of Carbon in H_2 and D_2, Respectively

T (K)	r (ng m^{-2} s^{-1})	r' (ng m^{-2} s^{-1})	r/r'
890	2.76	2.63	1.05
899	4.89	4.61	1.09
913	8.40	7.69	1.06
			1.07 ± 0.05

ported per unit initial surface area of carbon.

Temperature and pressure dependence of the rate are shown in Figs. 1–4 for the uncatalyzed and catalyzed reactions. By changing the space velocity it was checked that the rate of both reactions was not inhibited by methane. Extrapolation of the Arrhenius plot for the uncatalyzed reaction to lower temperatures indicates that the catalyzed reaction is about 2000 times faster than the uncatalyzed reaction at 890 K and atmospheric hydrogen pressure. Rate data for the uncatalyzed and catalyzed
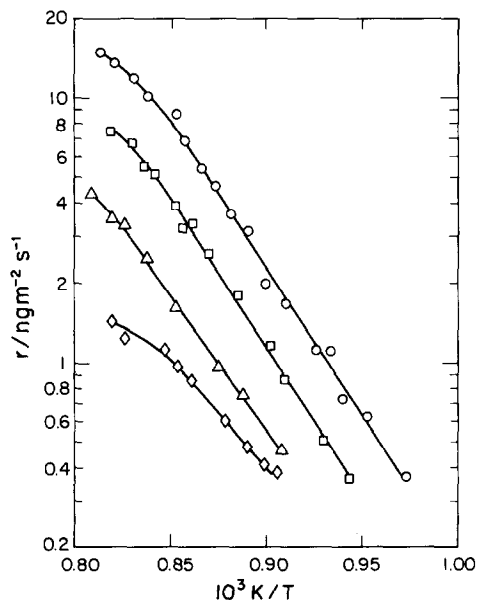
reactions of carbon H_2 and D_2 are shown in Tables 2 and 3.

DISCUSSION

General Kinetic Considerations

The Arrhenius plots for the uncatalyzed hydrogenolysis of carbon (Fig. 1) curve slightly at high temperatures as the reaction approaches equilibrium. The activation energy calculated from the plots at 49 kPa, 73 mol^{-1}. The reaction order is 1.41 ± 0.10 (Fig. 2). Both the activation energy and the reaction order fall into the range of activation energies (120–350 kJ mol^{-1}) and reaction orders (0.9–2.0) reported in the literature (1–5).

The Arrhenius plots for the platinum-catalyzed hydrogenolysis of carbon (Fig. 3) also curve to the left at high temperatures. Indeed, the plots peak and curve downward at still higher temperatures. This is due to the fact that the hydrogen and methane leaving the reactor at high temperatures are near equilibrium (dotted lines) and the equilibrium concentration of methane decreases with increasing temperature. Thus the decrease in rate at high temperatures repre-
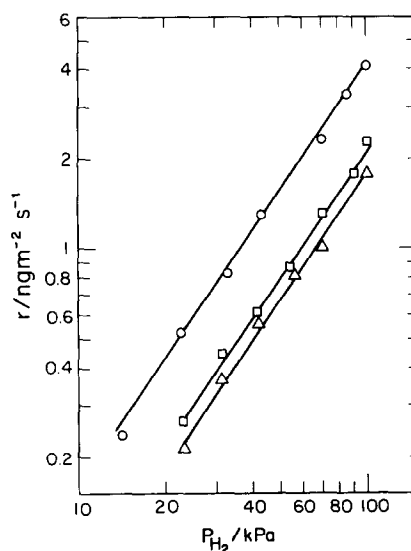

FIG. 1. Uncatalyzed hydrogenolysis of carbon: Arrhenius plot for the rate r of gasification of carbon. Pressure of H_2: ○, atmospheric; □, 73 kPa; △, 49 kPa; ◇, 28 kPa.

FIG. 2. Uncatalyzed hydrogenolysis of carbon: Dependence of rate r of gasification of carbon on pressure of H_2. Temperature: △, 1109 K; □, 1126 K; ○, 1165 K.
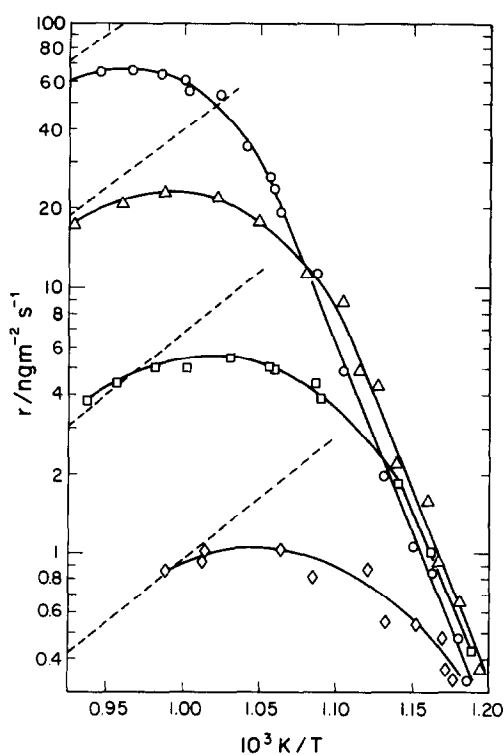
FIG. 3. Pt-catalyzed hydrogenolysis of carbon: Arrhenius plot for the rate r of gasification of carbon. Pressure of H_2: O, atmospheric; $\triangle$, 49 kPa; $\square$, 20 kPa; $\diamondsuit$, 7.2 kPa. Dotted lines represent the expected *net* rate if H_2 and CH_4 leaving the reactor are in equilibrium with carbon.

found. Our results show that the peaks in the Arrhenius plots of Rewick *et al.* were due neither to competing gasification and surface annealing reactions, as suggested by the authors, nor to pore diffusion as suggested by Marsh and Taylor (*9*), but rather to the approach of the reaction to chemical equilibrium at the reactor exit. Indeed, a calculation of the predicted net reaction rates at equilibrium from the parameters presented in the paper and a comparison to the reported results indicates that this is the case.

Rewick *et al.* calculated an activation energy of 230 kJ mol^{-1} for platinum-catalyzed hydrogenolysis of carbon. If only their points at low temperature and high hydrogen partial pressure (where the reaction is chemically controlled) are used, an activation energy of 250 ± 30 kJ mol^{-1} is obtained. There is excellent agreement between our activation energy of 260 ± 10 kJ mol^{-1} and the true activation energy of Rewick *et al.*

sents a decrease in the measured *net* rate, not a decrease in the *forward* rate of catalytic carbon hydrogenolysis. The activation energy calculated from the plots at low temperature for a hydrogen partial pressure of 20 kPa, 59 kPa, and atmospheric pressure is 260 ± 10 kJ mol^{-1}. At low temperatures and high hydrogen partial pressures, where the reaction rate is not influenced by the approach to equilibrium, the reaction is zero order (Fig. 4).

The platinum-catalyzed reaction yields a maximum in overall reaction rate as a function of temperature (Fig. 3) due to the approach of hydrogen and methane to equilibrium at high temperatures and low pressures. No anomalous peaks in the forward reaction rate as a function of temperature, as reported by Rewick *et al.* (*7*), were
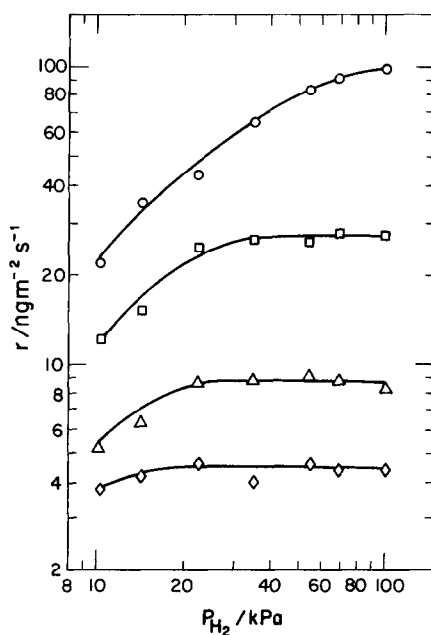

FIG. 4. Pt-catalyzed hydrogenolysis of carbon: Dependence of rate r of gasification of carbon on pressure of H_2. Temperature: $\diamondsuit$, 830 K; $\triangle$, 842 K; $\square$, 873 K; O, 905 K.
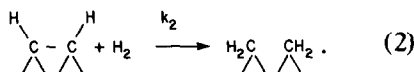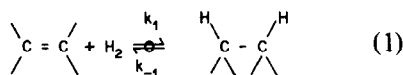
The reaction order of $\frac{1}{2}$ reported by Rewick et al. was calculated from the rates at hydrogen partial pressures of 1, 10, and 101 kPa. At the two lower pressures, the net rate is not equal to the forward rate due to the approach to equilibrium. The reaction is truly zero order, not $\frac{1}{2}$ order.

Finally, our result that the platinum-catalyzed reaction is zero order in hydrogen indicates that our rate is not influenced by pore diffusion (17). Walker et al. (18) have eloquently described the effect of pore diffusion on the kinetics of gas–carbon reactions. A measured zero order implies a true zero order of the chemical reaction. This is an important result since differences in reaction order and activation energy reported for gas–carbon reactions are often attributed to pore diffusion problems (18).

Besides, if pore diffusion does not influence rates in the catalyzed reaction, this conclusion is a fortiori true for our rates of the uncatalyzed reaction which were all smaller than for the catalyzed reaction.

Mechanism for Uncatalyzed Hydrogenolysis of Carbon

Only Zielke and Gorin (1) have proposed a mechanism for the uncatalyzed hydrogenolysis of carbon. In their model, the reaction takes place through consecutive steps, the first two of which are:

$$\overset{\backslash}{\underset{/}{C}} = \overset{/}{\underset{\backslash}{C}} + H_2 \underset{k_{-1}}{\overset{k_1}{\rightleftarrows}} \overset{H}{\underset{/\backslash}{\overset{\backslash}{C}}} - \overset{H}{\underset{/\backslash}{\overset{/}{C}}} \quad (1)$$

Clearly the first equilibrated step is hydrogenation while the second rate-determining one is hydrogenolysis. If the surface of the reacting carbon is mostly covered with the intermediate produced in the first step, steps following the second one and leading to methane are not significant kinetically. The rate of adsorption of hydrogen on graphite (19) and Spheron (14) has been

$$\overset{H}{\underset{/\backslash}{\overset{\backslash}{C}}} - \overset{H}{\underset{/\backslash}{\overset{/}{C}}} + H_2 \overset{k_2}{\longrightarrow} \underset{/\backslash}{H_2C} \quad \underset{/\backslash}{CH_2} . \quad (2)$$

found to fit the Elovich equation, suggesting that the activation energy for hydrogen adsorption is dependent on surface coverage. Hence the carbon surface appears to be nonuniform and nonuniform surface kinetics is preferred over uniform surface kinetics. Temkin (20) gives a general rate equation for two-step reactions on nonuniform surfaces with Elovich rates of adsorption,

$$r = \frac{k_1 k_2 P_{H_2}^2 - k_{-1} k_{-2}}{(k_1 P_{H_2} + k_{-2})^\alpha (k_2 P_{H_2} + k_{-1})^{(1-\alpha)}}, \quad (3)$$

where $0 \leq \alpha \leq 1$ is the Brønsted coefficient, frequently in the vicinity of $\frac{1}{2}$. If step (1) is equilibrated $(k_{-1} \gg k_2 P_{H_2})$ and the rate of the reverse reaction can be ignored $(k_{-2} \cong 0)$, the rate is given by:

$$r = k_2 \left(\frac{k_1}{k_{-1}}\right)^{(1-\alpha)} P_{H_2}^{(2-\alpha)}.$$

The reaction mechanism of Zielke and Gorin is consistent with reaction orders in hydrogen between 1 and 2. Our reaction order of 1.41 agrees with this model for $\alpha = 0.59$, a reasonable value and, as observed:

$$r = k P_{H_2}^{1.41}$$

with $k = k_2 K_1^{0.41}$ and $K_1 = k_1/k_{-1}$. The measured activation energy, E, is related to the activation energy of the rate-determining step, E_2, and the enthalphy of adsorption of hydrogen on carbon, ΔH_1, by

$$E = E_2 + 0.41 \Delta H_1.$$

The heat of adsorption of hydrogen on carbon has been measured to be between -60 and -230 kJ mol^{-1} in different investigations (19, 21, 22). The measured activation energy in this study is 215 kJ mol^{-1}. Thus, the activation energy for the rate-determining carbon–carbon bond-breaking step, E_2, is estimated to be between 240 and 310 kJ mol^{-1}.
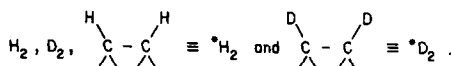
The kinetic isotope effect, r/r', where the prime represents D_2, for the uncatalyzed hydrogenolysis of carbon was found to be

1.12. The kinetic isotope effect expected from the mechanism of Zielke and Gorin can be estimated. There will be contributions to the kinetic isotope effect from both the rate constant of the rate-determining step, k_2, and the equilibrium constant for hydrogen adsorption on carbon, k_1.

$$\frac{r}{r'} = \frac{k_2}{k_2'}\left(\frac{K_1}{K_1'}\right)^{0.41}. \qquad (4)$$

At high temperatures, k_2/k_2' should be about $2^{1/2}$, the square root of the ratio of the molecular weights of deuterium and hydrogen, i.e., the so-called classical limit.

What will be the value of K_1/K_1'? An estimate can be made by estimating the partition functions Q of the various species involved,

$$H_2, D_2, \quad \underset{/\backslash}{\overset{H}{\underset{C}{\diagdown}}} - \underset{/\backslash}{\overset{H}{\underset{C}{\diagup}}} \equiv {}^*H_2 \quad \text{and} \quad \underset{/\backslash}{\overset{D}{\underset{C}{\diagdown}}} - \underset{/\backslash}{\overset{D}{\underset{C}{\diagup}}} \equiv {}^*D_2 .$$

Then

$$\frac{K_1}{K_1'} = \frac{Q(^*H_2)\,Q(D_2)}{Q(^*D_2)\,Q(H_2)}. \qquad (5)$$

First $Q(D_2)/Q(H_2)$ will be calculated.

$$\frac{Q(D_2)}{Q(H_2)} = \left(\frac{M_{D_2}}{M_{H_2}}\right)\left(\frac{I_{D_2}}{I_{H_2}}\right)^{3/2}$$
$$\left(\frac{1 - \exp(-h\nu_{H_2}/kT)}{1 - \exp(-h\nu_{D_2}/kT)}\right)$$
$$\left(\frac{\exp(-\tfrac{1}{2}h\nu_{D_2}/kT)}{\exp(-\tfrac{1}{2}h\nu_{H_2}/kT)}\right). \qquad (6)$$

The following information is available:

$$(M_{D_2}/M_{H_2}) = (I_{D_2}/I_{H_2}) = 2,$$
for the ratios of masses and moments of inertia;

$$\theta_V(H_2) = h\nu_{H_2}/k = 6215 \text{ K} \qquad (23);$$

$$\theta_V(D_2) = h\nu_{D_2}/k = 4394 \text{ K} \qquad (23).$$

Hence, at 1100 K,

$$Q(D_2)/Q(H_2) = 13.14. \qquad (7)$$

$Q(^*D_2)/Q(^*H_2)$ cannot be calculated exactly since spectroscopic data are not available. However, the ratio can be estimated.

For $^*H_2$ there are two C–H bonds, each of which has three vibrational degrees of freedom—one stretching and two bending. For protium bonded to carbon in general, it has been suggested (24) that the following values be used for the stretching and bending frequencies: stretching = 3000 cm^{-1}, bending = 2000 cm^{-1}. The stretching and bending frequencies for a carbon–deuterium bond can be calculated from

$$\nu_{C-D} = \left(\frac{\mu_{C-H}}{\mu_{C-D}}\right)^{1/2}\nu_{C-H}, \qquad (8)$$

where μ is the reduced mass and can be calculated for C–H and C–D bonds to be

$$\mu_{C-H} = 0.923 \text{ a.u.};$$

$$\mu_{C-D} = 1.714 \text{ a.u.}$$

Substituting into Eq. (8) yields

$$\nu_{C-D} = 0.734\nu_{C-H}.$$

The following values are calculated for vibrational temperatures for stretching and bending of C–H and C–D bonds:

stretching:

$$\theta_{vs}(C-H) = 4319 \text{ K}$$
$$\theta_{vs}(C-D) = 3170 \text{ K};$$

TABLE 4

Calculation of K_1/K_1' and r/r' as a Function of the Frequency of the Stretching and Bending of a C–H Bond Resulting from Hydrogen Adsorbed on Carbon

Relative frequency[a]	K_1/K_1'	r/r'
0.75	1.13	1.48
0.90	0.91	1.36
1.00	0.77	1.26
1.10	0.64	1.17
1.25	0.52	1.08

[a] Relative frequency defined as frequency/reference frequency. The bending and stretching frequencies for both C–H and C–D bonds are calculated by multiplying the reference frequency by the relative frequency. The reference frequencies used are: C–H stretching— 3000 cm^{-1}, C–H bending—2000 cm^{-1}; C–D stretching—2202 cm^{-1}, C–D bending—1468 cm^{-1}.

bending:

$\theta_{vb}(C-H) = 2880$ K

$$\theta_{vb}(C-D) = 2114 \text{ K}.$$

For $*H_2$ there are two C–H bonds, resulting in two stretching and four bending degrees of freedom.

$$\frac{Q(*D_2)}{Q(*H_2)} = \left(\frac{1 - \exp(-\theta_{vs}(C-H)/T)}{1 - \exp(-\theta_{vs}(C-D)/T)}\right)^2 \left(\frac{1 - \exp(-\theta_{vb}(C-H)/T)}{1 - \exp(-\theta_{vb}(C-D)/T)}\right)^4$$

$$\times \left(\frac{\exp(-\tfrac{1}{2}\theta_{vs}(C-D)/T)}{\exp(-\tfrac{1}{2}\theta_{vs}(C-H)/T)}\right)^2 \left(\frac{\exp(-\tfrac{1}{2}\theta_{vb}(C-D)/T)}{\exp(-\tfrac{1}{2}\theta_{vb}(C-D)/T)}\right)^4.$$

At 1100 K

$$Q(*D_2)/Q(*H_2) = 17.13.$$

Substituting the calculated values of $Q(D_2)/Q(H_2)$ and $Q(*D_2)/Q(*H_2)$ into Eq. (5) yields at 1100 K: $K_1(H_2)/K_1(D_2) = 0.77$.

From Eq. (4), the predicted kinetic isotope effect is then

$$r/r' = 1.26.$$

In order to test the sensitivity of the theoretical calculations to the vibrational frequencies of $*H_2$ used, the values of K_1/K_1' and r/r' have been calculated for vibrational stretching and bending frequencies from 0.75 to 1.25 times the reference frequencies, where the reference frequencies, which were used in the above calculations are: C–H stretching—3000 cm^{-1}, C–H bending—2000 cm^{-1}, C–D stretching—2202 cm^{-1}, C–D bending—1468 cm^{-1}. The results are given in Table 4.

What is the correct value for the vibrational frequencies of hydrogen adsorbed on carbon? The absorption of infrared radiation by bulk carbon makes this difficult to determine experimentally. However, the following range of frequencies have been noted for C–H stretching in gaseous hydrocarbons:

alkane	2850–2960 cm^{-1};
alkene	3020–3080 cm^{-1};
aromatic	3000–3100 cm^{-1};
alkyne	3300 cm^{-1}.

These are within 10% of the reference frequency used. The stretching frequency for hydrogen in *coke* formed from the catalytic cracking of *n*-pentane and isopentane vapors has been measured to be 3450–3300 cm^{-1} (25), as in alkynes, about 10% higher than our reference value. If hydrogen is similarly bound on carbon, the results of Table 4 show that the kinetic isotope effect will be less than 1.26, in the vicinity of the experimentally determined value of 1.12 ± 0.05.

Thus, both the reaction order in hydrogen of 1.41 and the kinetic isotope effect of 1.12 agree with the mechanism proposed by Zielke and Gorin (1). It would be interesting to obtain experimental vibration frequencies of C–H species on carbon surfaces by electron energy loss spectroscopy.

Mechanism of the Platinum-Catalyzed Hydrogenolysis of Carbon

Ever since hydrogen spillover was found to occur on carbon (8) and metallic oxides (26), it has been proposed in several reactions. The spillover mechanism for catalytic hydrogenolysis of carbon as proposed by Rewick et al. (7) has been described in the Introduction. Spillover was espoused as the reaction mechanism by Rewick et al. (7) because both platinum-catalyzed hydrogenolysis of carbon and atomization of dihydrogen to hydrogen by platinum (27) exhibited reaction orders in dihydrogen of ½ and similar activation energies. However, the reaction order of platinum-catalyzed hydrogenolysis of carbon has been determined in this investigation to be zero.

The basic premise on which the spillover

mechanism of catalytic carbon hydrogenolysis is based is that the supply of hydrogen atoms to the reactive sites of the carbon is the rate-determining step for the uncatalyzed hydrogenolysis. Yet, our kinetic study of the latter reaction led us to conclude that a carbon–carbon bond breaking step is rate determining. In addition, hydrogen adsorption on a clean carbon surface is much faster than carbon hydrogenolysis. Robell (14) found that hydrogen adsorption on 1% Pt/C was about ten times faster than on carbon at 573 K and decreased to about six times faster at 665 K at a hydrogen pressure of 8 kPa. It is unlikely that this small difference in adsorption rates could account for a 2000-fold increase in hydrogenolysis rates unless spilled-over hydrogen was present in a different form than adsorbed hydrogen.

We propose that the platinum-catalyzed hydrogenolysis of carbon does not occur by hydrogen spillover. Rather, the role of platinum seems to be to provide a lower activation energy step for the rate-determining breakage of carbon–carbon bonds resulting in the removal of a carbon atom from the carbon lattice with subsequent removal of this carbidic carbon atom as methane.

The expected kinetic isotope effect can be estimated. Since the reaction is zero order in hydrogen and the surface coverage of hydrogen on platinum or carbon is dependent on the hydrogen pressure, it is clear that the breakage of a hydrogen–hydrogen, hydrogen–carbon, or hydrogen–platinum bond does not occur when the carbon–carbon bond is broken by the interaction with platinum in the rate-determining step

$$\begin{array}{c}\diagdown \\ -C \\ \diagup\end{array} - \begin{array}{c}\diagup \\ C \\ \diagdown\end{array} \;+\; Pt \;\longrightarrow\; C - Pt \;+\; \begin{array}{c}\diagdown \diagup \\ C \\ \diagup \diagdown\end{array} .$$

Thus no primary kinetic isotope effect is expected; but the carbon surface may still be partially covered with adsorbed hydrogen, as in the case of the uncatalyzed reaction, leading to a secondary kinetic isotope effect. The observed kinetic isotope effect

of 1.07 is in the range expected for a secondary kinetic isotope effect (24).

The measured activation energy is then the true activation energy for the carbon–carbon breaking step. It is lower than the true activation energy for the carbon–carbon breaking step, E_2, in the uncatalyzed reaction. It is in excellent agreement with the activation energy calculated from the data of Rewick et al. (7) far from equilibrium. The reaction of carbon at the catalyst–carbon interface is supported by studies of catalyzed hydrogenolysis of carbon with optical microscopy (28) and controlled atmosphere electron microscopy (29, 30). The formation of channels on the basal plane of graphite by moving catalyst particles can be inferred from the micrographs. Reaction of carbon was only observed in the vicinity of catalyst particles. Uncatalyzed edge recession of channels was not observed. Controlled atmosphere electron microscopy studies of Pt (29) and Ni (30) indicate that large catalyst particles break up and redisperse during catalytic hydrogenolysis. Whether this occurs by surface transport of metal atoms or through dissolution of the metal in the carbon is unknown. The observation that large platinum particles carve channels in graphite at a faster rate than small platinum particles during catalyzed reaction (29) suggests that diffusion of carbon through the catalyst is not the rate-determining step.

CONCLUSIONS

All the data discussed above are consistent with the following statements. First, the rate-determining step for the uncatalyzed hydrogenolysis of carbon is a reaction between hydrogen and a hydrogen-covered carbon surface resulting in the breakage of a carbon–carbon bond.

The rate-determining step for the catalytic hydrogenolysis of carbon is the reaction of carbon with platinum resulting in the breakage of carbon–carbon bonds and the removal of a carbon atom from the carbon lattice. Although the catalyst also serves as

a source of adsorbed hydrogen atoms needed to convert carbon to methane, the supply of these hydrogen atoms, either through spillover of hydrogen from the platinum to the carbon or for a reaction at the platinum–carbon interface, is not the rate-determining step. The results suggest that the primary role of the catalyst is to break carbon–carbon bonds rather than to dissociate gas molecules for the catalyzed reaction of carbon with hydrogen and maybe with other gases as well.

ACKNOWLEDGMENT

REFERENCES

1. Zielke, C. W., and Gorin, E., Ind. Eng. Chem. 47, 820 (1955).
2. Blackwood, J. D., Aust. J. Chem. 15, 397 (1962).
3. Hedden, K., Z. Elec. 66, 652 (1962).
4. Hedden, K., in "Proceedings, 5th Conf. Carbon, Penn State, 1961" (S. Mrozowski, Ed.), pp. 125–131. Pergamon, Elmsford, New York, 1962.
5. Imai, H., Nomura, S., and Sasaki, Y., Carbon 13, 333 (1975).
6. Breisacher, P., and Marx, P. C., J. Amer. Chem. Soc. 85, 3518 (1963).
7. Rewick, R. T., Wentrcek, P. R., and Wise, H., Fuel 53, 274 (1974).
8. Robell, A. J., Ballou, E. V., and Boudart, M., J. Phys. Chem. 68, 2748 (1964).
9. Marsh, H., and Taylor, D. W., Fuel 54, 219 (1975).
10. Olander, D. R., and Balooch, M., J. Catal. 60, 41 (1979).
11. Balooch, M., and Olander, D. R., J. Chem. Phys. 63, 4772 (1975).
12. Tomita, A., and Tamai, Y., J. Catal. 27, 293 (1972).
13. Tomita, A., Sato, N., and Tamai, Y., Carbon 12, 143 (1974).
14. Robell, A. J., Ph.D. dissertation, University of California, Berkeley, 1964.
15. Amirnazmi, A., Benson, J. E., and Boudart, M., J. Catal. 30, 55 (1973).
16. Benson, J. E., and Boudart, M., J. Catal. 4, 704 (1965).
17. Weisz, P. B., and Prater, C. D., in "Advances in Catalysis and Related Subjects," Vol. 6, p. 143. Academic Press, New York, 1954.
18. Walker, P. L., Jr., Rusinko, F., and Austin, L. G., in "Advances in Catalysis and Related Subjects," Vol. 11, p. 133. Academic Press, New York, 1959.
19. Redmond, J. P., and Walker, P. L., J. Phys. Chem. 66, 1093 (1960).
20. Temkin, M. I., in "Advances in Catalysis and Related Subjects," Vol. 28, p. 173. Academic Press, New York, 1979.
21. Barrer, R. M., Proc. Roy. Soc. A 149, 253 (1935).
22. Barrer, R. M., J. Chem. Soc. 1256 (1936).
23. McQuarrie, P. A., "Statistical Mechanics," Harper & Row, New York, 1973.
24. Melander, L. C., "Isotope Effects on Reaction Rates," Ronald, New York, 1960.
25. Karmarka, K. H., and Natu, G. N., Spectrochim. Acta A 30, 547 (1974).
26. Khoobiar, S., J. Phys. Chem. 68, 411 (1964).
27. Brennan, D., and Fletcher, P. C., Trans. Faraday Soc. 56, 1662 (1960).
28. Tomita, A., and Tamai, Y., J. Phys. Chem. 78, 2254 (1974).
29. Baker, R. T. K., Sherwood, R. D., and Dumesic, J. A., J. Catal. 66, 56 (1980).
30. Keep, C. W., Terry, S., and Wells, M., J. Catal. 66, 451 (1980).